Research article

Techno-economic analysis of hydrogen enhanced methanol to gasoline process from biomass-derived synthesis gas

Malte Hennig [a,b], Martina Haase [b,*]

[a] *Karlsruhe Institute of Technology (KIT), Institute for Technical Chemistry (ITC), Herrmann-von-Helmholtz-Platz 1, 76344 Eggenstein-Leopoldshafen, Germany*
[b] *Karlsruhe Institute of Technology (KIT), Institute for Technology Assessment and Systems Analysis (ITAS), Karlstr. 11, 76133 Karlsruhe, Germany*

ABSTRACT

In this paper, the implications of the use of hydrogen on product yield and conversion efficiency as well as on economic performance of a hydrogen enhanced Biomass-to-Liquid (BtL) process are analyzed. A process concept for the synthesis of fuel (gasoline and LPG) from biomass-derived synthesis gas via Methanol-to-Gasoline (MtG) route with utilization of carbon dioxide from gasification by feeding additional hydrogen is developed and modeled in Aspen Plus. The modeled process produces 0.36 kg fuel per kg dry straw. Additionally, 99 MW electrical power are recovered from purge and off gases from fuel synthesis in CCGT process, covering the electricity consumption of fuel synthesis and synthesis gas generation. The hydrogen enhanced BtL procces reaches a combined chemical and electrical efficiency of 48.2% and overall carbon efficiency of 69.5%. The total product costs (TPC) sum up to 3.24 €/kg fuel. Raw materials (hydrogen and straw) make up the largest fraction of TPC with a total share of 75%. The hydrogen enhanced BtL process shows increased chemical, energy and carbon efficiencies and thus higher product yields. However, economic analysis shows that the process is un-profitable under current conditions due to high costs for hydrogen provision.

1. Introduction

Global energy demand has increased continuously in recent years. In 2017, about 80% of primary energy was generated from fossil fuels such as crude oil, natural gas and coal [1]. More than 35% of the energy is used for mobility applications, i.e. for shipping, aviation and road traffic [1]. The use of fossil raw materials for mobility is associated with the emission of large quantities of climate-affecting carbon dioxide (CO_2) which is the most abundant greenhouse gas (GHG), accounting for about two-thirds of GHGs in the atmosphere causing global warming [2].

With the revised version of the Renewable Energies Directive of the European Parliament and of the Council adopted in December 2018 (RED II for short) [3], the EU introduces the political framework for the use of renewable energy sources in the transportation sector for the time period from 2021 to 2030. This framework includes a minimum share of renewable energy sources in transportation of 14%, including a minimum share of 3.5% from advanced biofuels by 2030, and a limit on the quantity of conventional biofuels from food and feed crops to a maximum of 7%, and from used cooking oil (UCO) and animal fats of 1.7% [3]. According to [3], advanced biofuels encompass, amongst

others, biofuels produced from lignocellulosic biomass, e.g. residual straw and residues from forestry. These so-called second generation biofuels are regarded as one of the most promising renewable alternative to obtain liquid fuels for the transportation sector as they do not compete with food and fodder production and at the same time bear a high potential for greenhouse gas emission reductions [4]. In addition to ecological assessments of second generation biofuels, techno-economic assessments of new processes are necessary: by identifying critical process steps and parameters in terms of efficiency and costs, research and development can be directed to where major improvements can be achieved and economic feasibility be assessed [5]. Recent techno-economic analysis of processes for the production of second generation biofuels show, that production costs are currently higher compared to fossil fuels, mainly due to higher feedstock costs [5–7].

1.1. Synthetic fuels from biomass

One way of producing second-generation biofuels is the thermo-chemical conversion of lignocellulose, e.g. straw or wood, into synthesis gas by pyrolysis and gasification and subsequently to liquefied

petroleum gas (LPG) and gasoline [8]. To overcome the logistical and technical hurdles of the production of fuels from biomass instead of from fossil energy carriers, the bioliq® Biomass-to-Liquid (BtL) process is developed at Karlsruhe Institute of Technology (KIT) [9]. In this process, wheat straw is processed in decentralized pyrolysis plants into a well transportable slurry (biosyncrude) which has a significantly higher energy density compared to straw. This slurry is transported to a central high-pressure entrained flow gasifier for generation of synthesis gas [9–11].

Synthesis gas can be converted to a broad range of products by different processes that are well established in industry. Amongst these products are hydrogen (H_2), methane (CH_4), methanol (MeOH), and hydrocarbons (HCs), produced via Fischer-Tropsch or Methanol-to-Hydrocarbon synthesis [12,13]. Depending on process conditions chosen, methanol can be converted to different hydrocarbon products, yielding primarily aromatic compounds and alkanes within gasoline range (Methanol-to-Gasoline, MtG) or olefins (Methanol-to-Olefins, MtO) [14]. The bioliq® process employs a modified form of the MtG process, in which direct synthesis of dimethyl ether (DME) is used as intermediate stage in fuel production instead of methanol synthesis. This is advantageous as synthesis gas from the bioliq® gasifier already has a hydrogen/carbon monoxide (CO) ratio close to one which is favorable for DME synthesis [10,15].

1.2. Hydrogen-enhanced fuel synthesis

In the thermochemical conversion of biomass to synthesis gas for fuel production significant amounts of carbon leave the process unused in form of carbon dioxide [15,16] which is also true for the bioliq® process. One possibility for enhancement of carbon efficiency in gasification-based production of biofuels is the feeding of additional hydrogen for fuel synthesis, enabling the utilization of carbon dioxide contained in raw synthesis gas as feedstock material in order to increase product yield and thus carbon utilization and efficiency [7,16–18].

For production of hydrogen, different technologies already exist at industrial scale or are currently under development [19,20], amongst others, steam reforming of natural gas, electrolysis of water, and gasification of biomass. According to Wulf and Kaltschmitt [21], hydrogen production via alkaline and proton exchange membrane electrolysis using renewable electricity sources (i.e. from wind power) would be most favorable from an ecological perspective. Currently, electrolyzers are available in the MW scale. However, several projects have been announced that strive to close the gap towards the required 1000 MW scale by 2030 [22]. With increasing stack size lower costs for hydrogen provision can be expected [23].

The aim of this paper is to investigate the implications of the use of hydrogen on process performance regarding product yield, conversion efficiency and carbon utilization as well as on the economic performance of a hydrogen enhanced BtL process in comparison to the BtL process analyzed by Trippe et al. [15,24–26]. In terms of process modeling, the focus of this work is on the fuel synthesis (cf. Fig. 1). MtG process has been chosen for fuel synthesis as in contrast to Fischer-Tropsch synthesis, carbon dioxide can be used directly in methanol synthesis without prior conversion to carbon monoxide in an additional reverse watergas shift reactor (cf. [7]). Additionally, MtG yields a narrower product distribution in the LPG and gasoline range whereas Fischer-Tropsch products consist of gases, fuel (gasoline, kerosene, diesel), and waxes that require further processing [15]. A process concept for the large-scale synthesis of fuel from biomass-derived synthesis gas via MtG with utilization of carbon dioxide from gasification by feeding additional hydrogen is developed and modeled in Aspen Plus. The techno-economic analysis based on the results from process modeling encompasses the calculation of fuel (i.e. gasoline and LPG) production costs as well as the calculation of the operational result of the hydrogen enhanced BtL process.

2. Materials and methods

The examined hydrogen enhanced BtL process, i.e. the hydrogen enhanced MtG process and associated up- and downstream processes, is displayed in Fig. 1. The techno-economic analysis is done in three steps: Firstly, the process concept for hydrogen enhanced MtG synthesis is developed based on industrially well-established processes (cf. section 2.2) and subsequently implemented and modeled in the commercial flowsheeting software Aspen Plus V10 (section 2.3). Based on the results from fuel synthesis modeling together with mass and energy flows of upstream and downstream processes, the calculation of chemical and energy efficiency (section 2.4) and the economic process evaluation is carried out. The methods and input data utilized for estimation of investment, production costs and revenues are presented in section 2.5. A brief description of upstream processes for synthesis gas generation, of downstream processes for fuel gas utilization, and of provision of hydrogen and biomass (cf. Fig. 1), is given in section 2.1.

2.1. Upstream/downstream processes

The process for generation of synthesis gas from biomass, based on the bioliq® process concept, was modeled previously by Trippe et al. [15,24–26] and is used as starting point for the hydrogen enhanced MtG synthesis in this paper. In a first step, residual straw is converted to a slurry by means of fast pyrolysis[1] in a twin screw mixing reactor at 550 °C. Slurry for a 1000 MW entrained flow gasifier[2] is supplied by 11 decentral pyrolysis plants of 100 MW each and is transported over an average distance of 250 km. This requires a straw input (wet mass) of 284 t/h, and results in the generation of 192 t slurry per hour (cf. Fig. 1).

As in this paper, carbon dioxide from gasification is to be used as feedstock material in the hydrogen enhanced MtG synthesis, it is assumed that no carbon dioxide is separated from synthesis gas in the gas cleaning section. Thus, the mass flow of clean synthesis gas increases and its composition changes to 38.9% H_2, 47.7% CO, 13.4% CO_2 by volume while the modeling of the gasification process itself remains unaltered. Additionally, the gas composition for subsequent MtG synthesis is adjusted by the amount of hydrogen fed into the system instead of using water gas shift reaction.

Purge and off gases from methanol and fuel synthesis are used as fuel gas for energy recovery (electricity production) in a Combined Cycle Gas Turbine (CCGT) process according to [15,26] (cf. Fig. 1).

Hydrogen provision by alkaline electrolysis is accounted for based on the research of Wulf et al. [21,27,28]. In our paper, two alternatives are considered: one producing hydrogen off-site and the other producing hydrogen locally. This has consequences both on the cost of hydrogen provision as well as on how oxygen for gasification is supplied but does not affect the fuel synthesis process itself. When hydrogen is produced off-site, oxygen needs to be provided by air separation. Hydrogen is assumed to be transported via pipelines over an average distance of 400 km to the production site and is provided with a pressure of 7 MPa [21,27,28]. When hydrogen is produced locally, oxygen from electrolysis can be used and needs to be pressurized to gasification pressure (8 MPa) making air separation obsolete.

Biomass provision refers to provision of residual straw and includes straw collection and baling on agricultural areas as well as transport via tractor and trailer to decentralized pyrolysis plants over an average distance of 30 km according to Haase and Rösch [29].

2.2. Process description of hydrogen enhanced MtG synthesis

Hydrogen enhanced fuel synthesis consists of three subsystems: Methanol synthesis (A), hydrocarbon synthesis (B), and product

---

[1] Pyrolysis heat carrier: Steel balls, pyrolysis product recovery: 3 stage
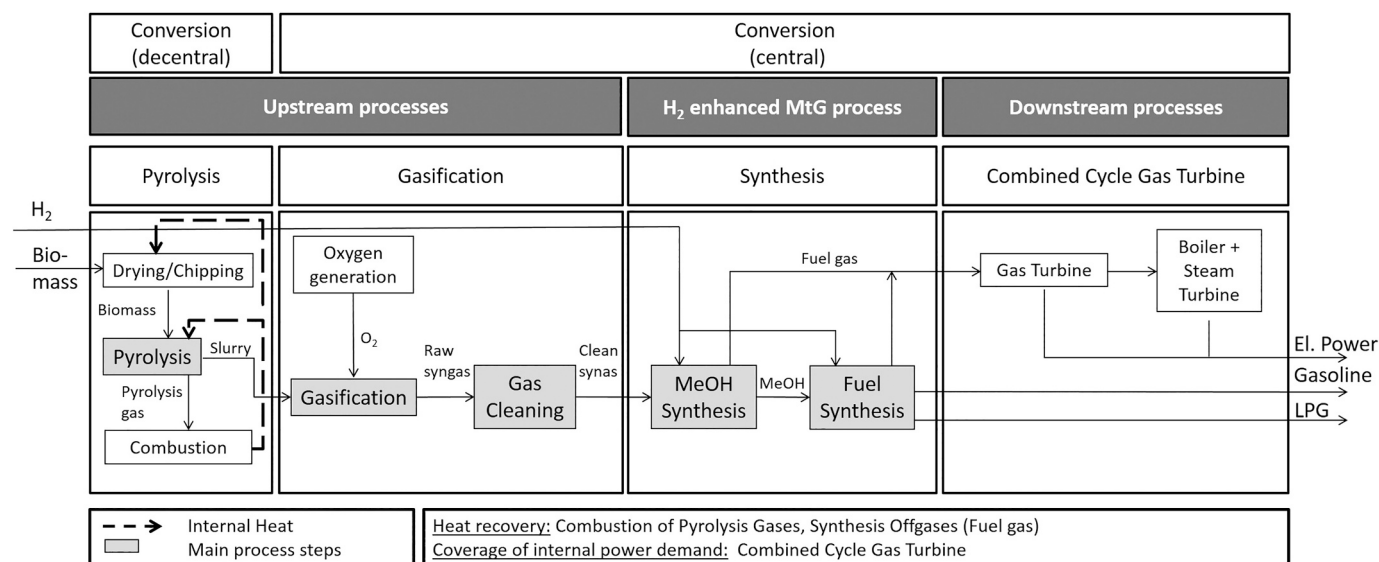[2] Operating pressure: 8 MPa, gasifying agent: oxygen

Fig. 1. Process chain of the hydrogen enhanced BtL process based on the bioliq® process concept (decentralized pyrolysis, centralized gasification and fuel synthesis).

recovery and purification (C). (B) and (C) are referred to as "fuel synthesis". The developed process flow diagram is shown in Fig. 2. The first step is the conversion of synthesis gas to methanol (section A in Fig. 2).

Methanol can be produced directly from carbon monoxide and carbon dioxide without need for prior conversion of carbon dioxide to carbon monoxide by reverse water gas shift reaction:

$$CO + 2\,H_2 \rightleftharpoons CH_3OH \tag{1}$$

$$CO_2 + 3\,H_2 \rightleftharpoons CH_3OH + H_2O \tag{2}$$

Synthesis gas from biomass-based slurries is hydrogen deficient for methanol synthesis. Therefore, additional hydrogen needs to be brought in to adjust the stoichiometric number (SN) as defined in Eq. (3). A slight hydrogen surplus is used to shift reaction equilibrium of methanol synthesis further to the product's side and achieve high methanol selectivity [30].

$$SN = \frac{[H_2] - [CO_2]}{[CO] + [CO_2]} \tag{3}$$

Due to thermodynamically limited per pass conversion of synthesis gas, industrial processes recycle unconverted synthesis gas to increase methanol yield. Large scale single train methanol plants with production capacities of 5000 tons per day typically operate three to four reactors in parallel [30,31].

Next, methanol is converted to hydrocarbons (section B in Fig. 2). Hydrocarbon product composition depends on reaction conditions, catalysts, and recycling of light product gases [32]. While a one-step process converting methanol directly to hydrocarbons is possible, a two-step process offers better temperature control by reducing adiabatic temperature rise in hydrocarbon synthesis, preventing cracking reactions and excessive formation of light olefins [33,34]. Therefore, in a first step methanol is dehydrated to a near equilibrium mixture of dimethyl ether, water, and unconverted methanol (Eq. (4)).

$$2\,CH_3OH \rightleftharpoons CH_3OCH_3 + H_2O \tag{4}$$

Next, this mixture is converted to hydrocarbons. Schematically, the formation of hydrocarbon chains (paraffins, olefins, aromatics) from previously unconverted methanol and DME can be written as [34].
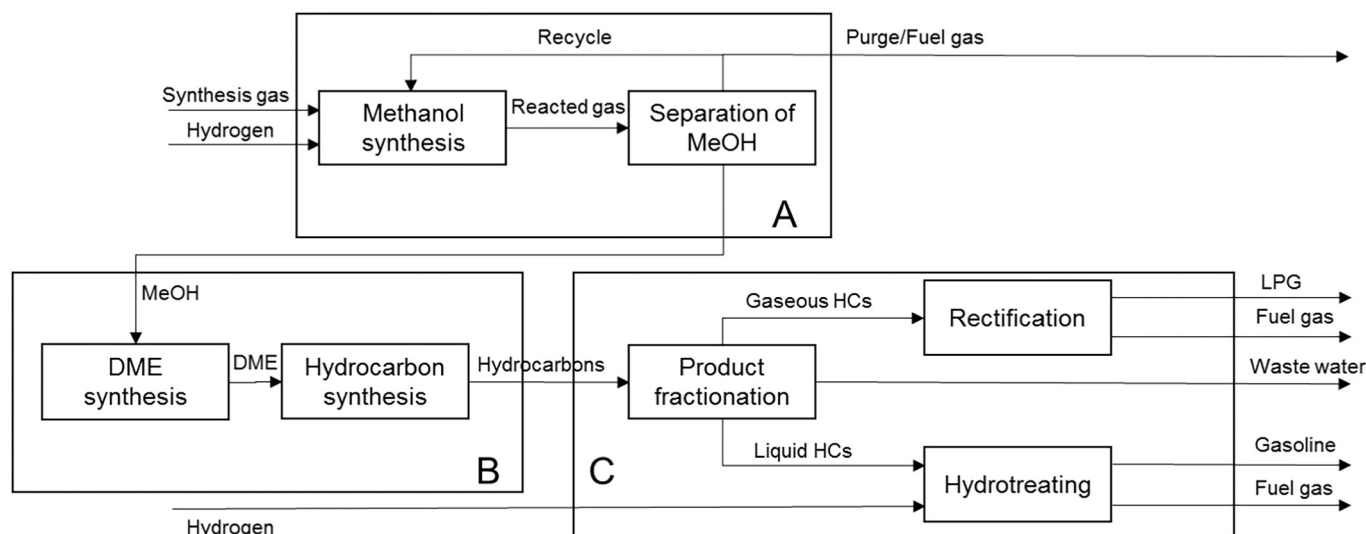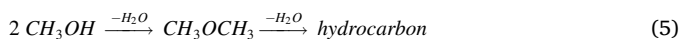

Fig. 2. Process flow diagram of the hydrogen enhanced MtG process: (A) methanol synthesis, (B) hydrocarbon synthesis, (C) product recovery and purification.

$$2\ CH_3OH \xrightarrow{-H_2O} CH_3OCH_3 \xrightarrow{-H_2O} hydrocarbon \qquad (5)$$

Even though coke formation is low in hydrocarbon synthesis, multiple fixed bed reactors that are operated in parallel are needed [35]. While the others are in operation, one will be regenerated by burning off coke.

In our model, two products, gasoline and LPG, are recovered from the hydrocarbons produced (section C in Fig. 2). Hydrocarbons are fractionated into a gaseous and a liquid fraction by condensation. LPG is recovered from the remaining gas phase by rectification, separating light and permanent gases. The liquid aqueous phase consisting of water formed during methanol synthesis and subsequent DME and hydrocarbon synthesis is removed. The organic liquid fraction is upgraded to gasoline by hydrotreating.

2.3. Modeling of hydrogen enhanced MtG process in Aspen Plus

The implementation of the previously described process in Aspen Plus is shown in the Appendix (Fig. A1.1). A summary of the most important material flows (composition, pressure, temperature, chemical energy) is given in the supplementary material. Throughout the model, Peng-Robinson equation of state with Gibbons-Laughton Alpha Function is used for thermodynamic calculations. This equation of state is recommended for refinery operations by Aspen Plus. The Gibbons-Laughton Alpha Function takes into account non-ideality of polar compounds [36], making it suitable for modeling of methanol synthesis also. A preliminary heat integration is implemented based on pinch analysis. Use of waste heat for generation of electricity or district heating is not considered in energy efficiency analysis. Within the subsequent subsections, key figures of the process model are given.

2.3.1. Methanol synthesis

Synthesis gas is converted to methanol within a reaction loop. The methanol synthesis reactor is modeled with a combined RPlug reactor model consisting of a first adiabatic unit and a second isothermal unit. Synthesis gas enters the first unit at a pressure of 6.0 MPa and 483 K. Each unit is sized by design specs in Aspen Plus so that the gas temperature at the outlet of the first unit is 503 K and the combined residence time of both units, calculated as gas hourly space velocity (GHSV), is equal to 10,000 h^{-1}. Reaction kinetics for modeling methanol synthesis have been taken from literature [37,38]. As methanol selectivity in industrial processes is above 99% [30], formation of side products is neglected within this work. The influence of pressure drop across the reactor is taken into account by applying Ergun's equation based on catalyst specifications from [38]. The reactor effluent is cooled to 313 K and partially condensed at a pressure of 5.6 MPa. Unconverted synthesis gas is recompressed and recycled with a purge ratio of 2% to achieve high methanol yield. Liquid raw methanol, separated from the reactor effluent, is depressurized to 3.4 MPa, degassed, and fed to subsequent hydrocarbon synthesis.

2.3.2. Hydrocarbon synthesis

Methanol is evaporated and preheated to 473 K and enters the DME synthesis reactor. The feed is further heated internally to the reactor temperature of 523 K by reaction heat. The gas phase dehydration reaction is modeled using Aspen Plus' REquil reactor model, calculating chemical equilibrium composition based on minimization of free Gibbs enthalpy. A temperature approach of 10 K is chosen to account for near equilibrium conversion of methanol to DME [26]. Before entering the gasoline synthesis reactor, the reactor feed is preheated to 613 K. Reaction takes place at 653 K and 3.3 MPa. The reactor is modeled with a RYield type reactor model. As a once-through process is employed within this study and reaction temperature is comparable, a product distribution based on the experimental work of Chang and Silvestri [34,39] is used (see Table 1).

Regarding aromatic content, this product distribution is similar to the

Table 1
Hydrocarbon product distribution in % (mass fraction) based on Chang and Silvestri [39].

Phase		Mass fraction in %	
Gas fraction		**44.9**	
	Propane		36.1
	Butane (n + i)		54.1
	Other		9.8
Liquid fraction		**55.1**	
	Alkanes		24.3
	Olefins		0.9
	Aromatics		74.8

product distribution determined from gasoline produced by the bioliq® process on a pilot scale [40] which employs a similar process as modeled in this paper. Full conversion of methanol and DME can be achieved [39]. For modeling purposes, structural isomers of aromatic compounds as o-, m-, p-xylene are lumped together. To assure that atom balances for C, H, and O are maintained within the hydrocarbon synthesis reactor model, stream composition of the gasoline synthesis reactor effluent is calculated in an Excel subroutine, assuming formation of low amounts of hydrogen and carbon dioxide. Of the total hydrocarbons formed, 55.1% by weight are in the C_{5+} gasoline range with an aromatic share of 74.8%. 95.3% of lighter hydrocarbons are within LPG range. MtG is less susceptible to coke formation than MtO with coke yielding <0.2% of methanol feed [41]. It is therefore neglected in terms of product distribution but considered in the choice of process equipment (cf. 2.2).

2.3.3. Product recovery and purification

After hydrocarbon synthesis, the reactor effluent is cooled to 313 K and liquid and gaseous phase are separated. Water is separated from the liquid organic phase. Light hydrocarbons < C_5 dissolved in the organic liquid phase will cause the gasoline's vapor pressure exceed permissible values specified in the European Standard for automotive fuels [42]. Therefore, those are separated by rectification in a degassing column at 1.0 MPa. The top product is recompressed to 1.5 MPa, mixed with the gas phase from first phase separation and fed into the LPG separation column operating at 1.5 MPa. At the top, light gases outside the LPG range are drawn off while the bottom product is LPG.

As aromatic content in gasoline is limited to 35% by volume [42] the bottom product from degassing column cannot be used directly as gasoline but must be treated further by hydrotreating or separation of aromatics or mixed with low aromatic fuels to comply with regulations. Within this study, hydrogenation is chosen to produce a fuel that is fully compliant with all regulations. Hydrogenation is carried out in a reaction loop, recycling surplus hydrogen. Data for hydrogenation of mixed aromatics free of sulfur is scarce in literature. Relatively mild reaction conditions of 513 K and 3.4 MPa are chosen, according to Wilson et al. [43]. The amount of hydrogen fed into the hydrotreating reaction loop is determined by a design specification adjusting the ratio of hydrogen to raw gasoline at 3000 scf/bbl (534.3 m^3/m^3). Hydrogen consumption is calculated based on conversion of 60% of aromatic compounds, sufficient to meet the 35% target, and full conversion of olefines to their corresponding fully hydrogenated specie. The calculated stream composition does not reflect the product distribution that would be expected based on thermodynamic calculations or reaction kinetics but is suitable for estimating hydrogen consumption. After hydrotreating, the reactor effluent is condensed at 313 K. The hydrogen rich gas phase is recycled, purging 5%. The gasoline is depressurized to 0.1 MPa and degassed.

2.4. Calculation of chemical and energy efficiency

Energy flows in terms of chemically bound energy are calculated based on the mass flows' composition and the corresponding higher heating value (HHV). As HHVs are not available for all hydrocarbon products considered in modeling, they are estimated according to Boie's

method on the basis of the elemental composition (carbon/hydrogen/oxygen) (cf. [13]). Detailed stream compositions are given in the supplementary material. The chemical efficiency η_{ch} is calculated based on energy content of products and educts:

$$\eta_{ch} = \frac{\sum \dot{m}_{Product,i} \; HHV_{Product,i}}{\sum \dot{m}_{Educt,i} \; HHV_{Educt,i}} \qquad (6)$$

The combined chemical and electrical efficiency $\eta_{comb.}$ takes into account the surplus net electricity $\dot{P}_{el,net}$ generated in CCGT process also:

$$\eta_{comb.} = \frac{\sum \dot{m}_{Product,i} \; HHV_{Product,i} + \dot{P}_{el,net}}{\sum \dot{m}_{Educt,i} \; HHV_{Educt,i}} \qquad (7)$$

When evaluating chemical and electrical efficiency of the hydrogen enhanced BtL process including upstream and downstream processes, the electrical power $\dot{P}_{Electrolysis}$ for hydrogen production and hydrogen compression needs to be included. Electrolysis requires a power input of 50.85 kWh/kg plus an addtional 1.27 kWh/kg for hydrogen compression [28,44], resulting in an electrolysis efficiency of 76.2% based on HHV.

2.5. Economic evaluation

For economic assessment, manufacturing costs *(MC)* per kilogram product, i.e. fuel (gasoline plus LPG), total product costs *(TPC)* as well as the operational result (calculated as Earnings before interests and taxes (EBIT) and Earnings before taxes (EBT)) of the hydrogen enhanced BtL process are calculated. The calculations are based on the methods for estimation of fixed capital investment *(FCI)* and total product costs *(TPC)* outlined by Peters and Timmerhaus [45]. Cost components and underlying assumptions for economic evaluation are summarized in Table 2.

As mentioned above, two alternatives – off-site production of hydrogen with delivery by pipeline and on-site generation of hydrogen are evaluated, differing in cost of hydrogen provision as well as investment and electricity consumption for supply of oxygen for gasification.

2.5.1. Investment estimation

The FCI for the hydrogen enhanced MtG process plant and downstream CCGT process is calculated based on the cost estimation of main plant components. In analogy to [53], the investment I_g for standardized equipment as heat exchangers (HX), separation columns, compressors etc. is estimated with the commercial software Aspen Capital Cost Estimator based on modeled mass and energy flows from flowsheet simulation. As reactors are much more unique in design, investment I_g for reactors is calculated from base investment I_0 available in literature for base capacity Cap_0. This is scaled to the respective capacity Cap_g needed by degression method [45]:

$$I_g = I_0 \left(\frac{Cap_g}{Cap_0} \right)^y \qquad (8)$$

Non-linearity of the investment-capacity correlation is taken into account by degression exponent y. As base years and currency differ, the reference investment is updated to € 2018 with cost development data of chemical plants from [54] and currency exchange rates for the corresponding year [55]. References for base investment for reactors of MtG and CCGT process are summarized in Table 3.

Associated costs as e.g. for secondary components are accounted for with ratio factors f_i for direct ($f_1 = 2.60$) and indirect ($f_2 = 1.44$) costs, specified in [15,45] for fluid processing plants.

$$FCI = I_g \left(1 + \sum_{i=1}^{2} f_i \right) \qquad (9)$$

Data for FCI of upstream processes is taken from [15,24–26] and updated to base year 2018 accordingly, resulting in FCI of 422.9 M€ for decentralized pyrolysis plants and 339.9 M€ for gasification without air separation and 438.6 M€ including air separation (cf. Table A2.1).

Table 2
Assumptions for economic evaluation of the hydrogen enhanced BtL process.

Category		Value	Unit	Source
Manufacturing costs				
Fixed costs				
	Depreciation period	15	a	Own assumption
	Annual operating hours	7008	h	[15,24,25]
	Interest rate	7	%	[45]
	Working capital	5	% of FCI	[45]
	Taxes	2	% of FCI	[45]
	Insurance	1	% of FCI	[45]
Variable costs				
	Raw materials			
	Straw	71	€/t dry mass	Own calculations based on [46]
	Hydrogen (off-site generation)	8190	€/t	[27]
	Hydrogen (on-site generation)	8096	€/t	[27]
	Operating labor	29.6	M€/a	[15,24,25]
	Utilities			
	Transport slurry	29	€/t	[29,47]
	Electricity	44.40	€/MWh	[48]
	Cooling water	0.043	€/m3	[49]
	Catalysts			
	Methanol synthesis	18.10	€/kg	[35]
	DME synthesis	19.25	€/kg	[35]
	Hydrocarbon synthesis	57.54	€/kg	[35]
	Hydrogenation	28.93	€/kg	[50]
	Wastewater treatment	2.00	€/m3	[49]
	Refrigeration (-50 °C)	50.85	€/GJ	[45]
	Maintenance and repairs			
	Methanol synthesis	4	% of FCI for individual process	[15,24,25,45]
	Fuel synthesis	6		
	Product recovery	3		
	CCGT	2		
	Operating supplies	15	% of maintenance and repairs	[45]
Plant Overhead		50	% of operating labor and maintenance and repairs	[45]
General expenses				
	Administration	15	% of operating labor	[45]
	Marketing and sales	2	% of TPC	[45]
	Research and development	5	% of TPC	[45]
Revenues				
	Electricity	44.40	€/MWh	[48]
	Gasoline	562	€/t	[51]
	LPG	420	€/t	[52]

2.5.2. Total product costs

According to [45], total product costs comprise manufacturing costs *(MC)* and general expenses *(GE)* as well as revenues from by-products *(RV$_{by}$)*. Manufacturing costs consist of fixed costs *(FC)*, variable costs *(VC)*, and plant overhead *(PO)* (cf. Eq. (10) and Table 2).

$$TPC = FC + VC + PO + GE - RV_{by} \qquad (10)$$

2.5.2.1. Fixed costs.
Fixed costs consist of depreciation, capital costs, and costs for taxes and insurance. Linear depreciation of FCI over a period of 15 years is assumed (cf. Table 2). Capital costs, i.e. interests, are estimated using half of the sum of FCI plus working capital *(WC)* at an interest rate of 7% (cf. [45,58]). Costs for taxes and insurance are calculated as

Table 3
Base capacities, base investments and degression exponents for reactors of hydrogen enhanced MtG and CCGT processes.

Description	Base Capacity Cap_0	Unit	Base Investment I_0 in k€ 2018	Degression Exponent y	Source
Hydrogen enhanced MtG					
Methanol synthesis					
Methanol reactor	10.2	t MeOH/h	629.9	0.60	[56]
Hydrocarbon synthesis					
DME synthesis reactor beds	39.8	t/h	609.8	0.57	[56]
DME synthesis reactor intercooler	37.2	MW$_{th}$	2031.7	0.65	[56]
Gasoline synthesis reactor beds	14.8	t DME-equiv./h	89.4	0.60	[56]
Gasoline synthesis reactor intercooler	37.2	MW$_{th}$	2031.7	0.65	[56]
Product recovery and purification					
Hydrogenation reactor	0.93	t raw gasoline/h	694.3	0.70	[57]
CCGT					
Gas turbine	91.7	MW$_e$	11,523.3	0.75	[26]
Steam generator	110.4	MW$_{th}$	7412.8	1	[26]
Steam turbine	48.5	MW$_e$	10,926.5	0.67	[26]

percentages from FCI (2 and 1% respectively) [45] (cf. Table 2).

2.5.2.2. Variable costs. Variable costs of the hydrogen enhanced MtG process comprise costs for raw materials (straw[3] and hydrogen), operating labor, utilities (transport of slurry[4], electricity, cooling water, catalysts, wastewater treatment, refrigeration)[5], maintenance and repairs, and operating supplies. For the hydrogen enhanced MtG process, costs for upstream processes (pyrolysis, gasification) can be summarized as costs for synthesis gas provision resulting in TPC of 273 €/t synthesis gas and MC of 251 €/t synthesis gas (€ 2018). Costs for raw materials and utilities are calculated based on mass and energy balances from flow-sheet simulation for hydrogen enhanced MtG synthesis together with their specific costs/prices (cf. Table 2). Corresponding mass and energy flows for upstream processes as well as costs for operating labor are taken from [15,24–26,29]. Costs for maintenance and repairs are calculated as percentages from FCI (cf. Table 2). Costs for operating supplies are calculated as percentages from costs for maintenance and repairs (cf. Table 2).

2.5.2.3. Plant overhead and general expenses. Plant overhead costs comprise e.g. costs for medical, safety, and restaurant facilities and are calculated as percentage of costs for labor and costs for maintenance and repairs [45] (cf. Table 2). General expenses consist of costs for administration, marketing and sales, and research and development. Costs for administration are calculated as percentage from operating labor costs (cf. Table 2). Costs for marketing and sales and research and development are calculated as percentage of TPC (cf. Table 2).

2.5.2.4. Revenues. Revenues for by-products, i.e. revenues for electricity, are calculated using the average wholesale electricity price for 2018 (44.04 €/MWh) from [48] (cf. Table 2). As electricity is produced in surplus, cost of electricity is charged as opportunity cost at the same price. Revenues from main products LPG and gasoline are calculated using expected selling prices given in Table 2. Selling price for gasoline refers to average gasoline manufacturing costs for 2018 of about 0,42 €/l taken from [51]. Selling price for LPG is based on LPG manufacturing costs for 2018 of about 0.25 €/l taken from [52].

3. Results and discussion

In this section, results for process efficiencies as well as the techno-economic analysis of the modeled hydrogen enhanced MtG process are presented and discussed.

3.1. Process efficiencies

The mass, carbon, and energy balances of the hydrogen enhanced MtG synthesis and of the hydrogen enhanced BtL process are visualized in Fig. 3. Mass and energy flows of the modeled process as well as the carbon contained in those streams are summarized in Table 4. Furthermore, chemical, combined chemical and electrical, and carbon efficiency are given in Table 4. Results from Trippe et al. [15] for gasoline synthesis via DME synthesis without utilization of carbon dioxide from gasification (and without use of additional hydrogen) and for the corresponding BtL process are included in Table 4 for comparison.

The modeled hydrogen enhanced MtG process produces 50.8 t/h gasoline and 36.4 t/h LPG. This translates into a product yield of 0.36 kg fuel per kg dry straw. 99.4 MW electrical power are recovered from purge and off gases from fuel synthesis in CCGT process, covering the consumption of fuel synthesis and synthesis gas generation. This results in a combined chemical and electrical efficiency of 48.2% for the complete process chain. When hydrogen is produced on-site, oxygen from electrolysis can be used for gasification. While the amount of LPG and gasoline produced does not change, the electric energy consumed in upstream process step gasification decreases by 31 MW[6], increasing surplus electrical energy to 59 MW. Thus, combined chemical and electrical efficiency increases to 49.4%. In both cases, energy released in form of heat accounts for the biggest loss in energy efficiency (cf. Fig. 3, middle). Due to reaction thermodynamics, this loss cannot be avoided completely. However, approximately 240 MW of reactor waste heat from hydrogen enhanced MtG process at a temperature level above 200 °C are available for energy recovery beyond internal heat demands, e.g. for electricity generation or district heating depending on actual site infrastructure.

The overall carbon efficiency of the hydrogen enhanced BtL process reaches 69.5%. As can be seen from Fig. 3 (bottom), carbon losses from fuel synthesis consist of light hydrocarbons outside the gasoline and LPG product range and purge gas from methanol synthesis. They account for only 8.4% of the total carbon initially contained in biomass. The biggest loss of carbon (21.3%) is due to the decentralized pyrolysis step. The pyrolysis gas can only be used for heating of the individual pyrolysis units but cannot serve as feedstock for the central gasification and subsequent fuel synthesis.

The purge ratios of methanol synthesis and hydrogenation were evaluated in terms of impact on carbon and chemical efficiency. While the hydrogenation purge ratio shows hardly any impact on both efficiencies, the methanol synthesis purge ratio does affect carbon and chemical efficiency. For a purge ratio of 1 to 5%, chemical efficiency of fuel synthesis decreases from 66.9% to 63.4% and carbon efficiency

---

[3] Input for upstream process pyrolysis
[4] Input for upstream process gasification
[5] Costs for natural gas (auxiliary burner for gasifier) and costs for emission reductions (SO$_2$ emissions from burning of pyrolysis gar) are neglected

[6] Difference between power savings from air separation (34.7 MW according to [26]) and additional power for compression of oxygen from electrolysis pressure to gasification pressure (3.4 MW according to own calculation)
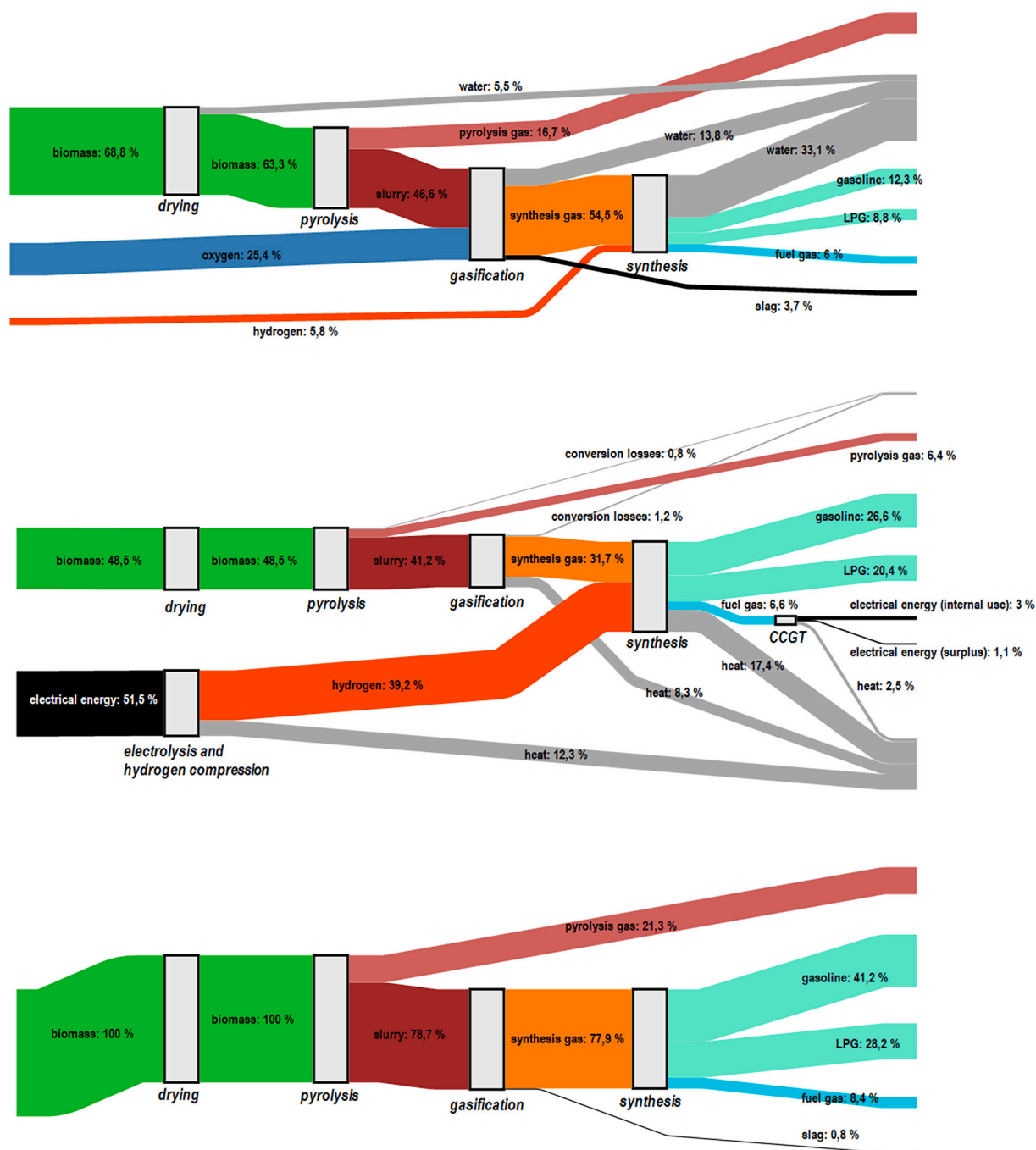
Fig. 3. Sankey diagrams of mass (top), energy (middle), and carbon (bottom) flows of hydrogen enhanced BtL process with off-site generation of hydrogen.

from 90.2% to 85.2% with increasing effect at higher purge ratios. The combined chemical and electric efficiency will be less affected due to increased energy recovery from purge gas with increasing purge ratio.

3.1.1. Discussion of process efficiencies

Dietrich et al. have conducted a similar study investigating different process configurations for production of fuel via Fischer-Tropsch process from biomass, power, and a combination thereof [7]. Hannula chose a similar approach as Dietrich et al., modeling a centralized gasifier with direct gasification of biomass but applying MtG process for conversion of synthesis gas to methanol and subsequently to gasoline [17]. In contrast to this study and Trippe et al. [15,24–26], Dietrich et al. [7] and Hannula [17] model a fully centralized process. However, the results regarding chemical efficiency of hydrogen enhanced BtL processes are very similar

when converted to LHV basis[7]. Differences can be explained by different product distribution of MtG synthesis and Fischer-Tropsch synthesis, and minor differences in process conditions chosen. In comparison to Dietrich et al. [7], carbon efficiency in this work is 28% lower. Hannula reaches a carbon efficiency of 88% for the centralized hydrogen enhanced BtL process when also considering LPG product [17]. The difference to both Dietrich et al. and Hannula is almost entirely due to the decentralized pyrolysis process, preventing the further use of a significant fraction of carbon contained in pyrolysis gas. In comparison to Hannula, the calculated synthesis carbon efficiency for the modeled hydrogen enhanced MtG psynthesis is almost identical. Therefore, it can be concluded that the

---

[7] This work: 53.0%; Dietrich et al.: 51.4% [7]; Hannula: 49.7% [17]

Table 4

Mass, carbon, and energy flows of hydrogen enhanced MtG synthesis and resulting hydrogen enhanced BtL process (with utilization of carbon dioxide from gasification) and of gasoline synthesis via DME and BtL process (without utilization of carbon dioxide from gasification).

Streams and Efficiencies	Hydrogen enhanced MtG synthesis			Gasoline via DME synthesis Trippe et al. [15]		
	Mass in t/h	Carbon in kmol/h	Energy in MW	Mass in t/h	Carbon in kmol/h	Energy in MW
Input						
Clean synthesis gas[a]	225	6858	771	144	4799[b]	758
Hydrogen (MeOH synthesis)	22.6	0	896	-	-	-
Hydrogen (hydrotreating)	1.4	0	56.5	-	-	-
Electricity	-	-	5.8	-	-	5.6
Output						
Gasoline	50.8	3631	645	30.0	2139[c]	394
LPG	36.4	2485	496	-	-	-
Gross electricity generation	-	-	99	-	-	131
Process efficiencies	Hydrogen enhanced MtG synthesis	Hydrogen enhanced BtL		Gasoline via DME synthesis Trippe et al. [15]	BtL Trippe et al. [15]	
	Efficiency in %			Efficiency in %		
Chemical efficiency	66.3[d]	47.0[d]		51.9	33.5	
Combined chemical and electrical efficiency	71.7[d]	48.2[d]		68.5	38.6	
Carbon efficiency[e]	89.2	69.5		44.6	24.3	

[a] Composition in % by weight: 3.9% H_2, 66.6% CO, 29.5% CO_2.

[b] Own calculation.

[c] Own calculation based on assumed average H:C molar ratio of 2 for gasoline.

[d] Required power of alkaline electrolysis: 1,250 MWe (i.e. efficiency of 76.2 % based on HHV taken from Wulf et al. 2018 [28], Koj et al. 2017 [44]; required power of synthesis gas generation: 65.9 MW taken from Trippe 2013 [26]; Chemical energy of biomass: 1,177 MW [26].

[e] Carbon input to pyrolysis from biomass: 8,803 kmol C/h taken from Trippe et al. 2010 [24], Trippe 2013 [26].

results from modeling of the hydrogen enhanced MtG synthesis are plausible and in good agreement with existing literature.

The BtL process modeled by Trippe et al. with identical biomass input and gasifier reaches a combined chemical and electrical efficiency of 38.6% [15]. Due to differences in product composition for hydrocarbon synthesis the higher combined chemical and electrical efficiency cannot be ascribed solely to the use of additional hydrogen but also to the better utilization of the hydrocarbon spectrum when introducing LPG as an additional product. This leads to a smaller amount of hydrocarbons being rejected to CCGT process, increasing overall process efficiency. Additionally, methanol synthesis with recycling of unconverted synthesis gas leads to a higher synthesis gas conversion in comparison to the once-through DME synthesis employed in the unmodified BtL process. This leads to an additioanl increase in product yield and thus in process efficiency. The carbon efficiency of the hydrogen enhanced BtL process is almost tripled in comparison to Trippe et al. [15]. This effect is due to the utilization of carbon dioxide from gasification and prevents the loss of 24% of carbon input. Therefore, product yield increases from 0.12 to 0.36 kg fuel per kg dry straw.

The comparison with Trippe et al. [15,24–26] on the one hand and Hannula [17] and Dietrich et al. [7] on the other shows that the additional use of hydrogen is suitable for increasing product yield in comparison to BtL processes without use of hydrogen. However, due to the decentralized pyrolysis step the product yield and thus carbon efficiency cannot be as high as for a completely centralized process. At the same time, energy efficiency is not affected by the decentralized pyrolysis as energy efficiencies are merely the same for all hydrogen enhanced BtL processes.

3.2. Economic analysis

The economic evaluation of the hydrogen enhanced BtL process is based on estimation of fixed capital investment and the calculation of manufacturing and total product costs. The economic viability is assessed based on the operational result that would be expected for a large-scale realization assuming current market prices for gasoline and LPG. If not stated differently, off-site hydrogen generation is assumed. For on-site

hydrogen production, reduced costs for hydrogen provision (no hydrogen transport costs), lower investment (no air separation unit needed) and in total reduced electrical power consumption (additional electricity demand for compression of oxygen from on-site electrolysis to gasification pressure but no electricity demand for air separation unit) are considered.

3.2.1. Estimation of Fixed Capital Invest (FCI)

The fixed capital invest (FCI) for the hydrogen enhanced BtL process, consisting of pyrolysis (11 decentralized pyrolysis units of 100 MW each), gasification (one central high pressure entrained-flow gasifier of 1000 MW), fuel synthesis, and CCGT plant for energy recovery totals 1198 M€. A detailed list of capacities and corresponding FCI for all main components is given in Table A2.1 in the Appendix. The largest share of FCI is for upstream processes pyrolysis and gasification (72%). Methanol synthesis (9%), hydrocarbon synthesis (7%), product recovery and purification (5%), and CCGT plant (7%) account for a total share of 28% of FCI. Reactors comprise about 57% of FCI of hydrogen enhanced MtG process, followed by the heat exchanger network (23%) and compressors (12%). When hydrogen is provided on-site by alkaline electrolysis, FCI is reduced by 91 M€ as oxygen is co-generated and no air separation unit is needed, leading to a reduction of FCI by 7.6%.

3.2.2. Total product costs and operational result

With an annual operating time of 7008 h, the yearly production of fuel is 611,600 t (356,300 t/a gasoline, 255,300 t/a LPG). The total product costs of the hydrogen enhanced BtL process (off-site H₂ production) sum up to 3.24 €/kg fuel, and manufacturing costs sum up to 3.00 €/kg fuel. A detailed summary of all costs on a yearly base is given in Table 5 while Fig. 4 shows the distribution of costs per kilogram fuel.

Raw materials (hydrogen and straw) make up the largest fraction of TPC with a total share of 75% though cost of hydrogen is the single largest cost contributor by far (69% of TPC). When hydrogen is produced on-site, TPC is reduced to 3.16 €/kg fuel. Savings are due to lower electricity consumption (no air separation unit) i.e. higher revenues from surplus electricity and reduced costs for hydrogen (no transport

costs). Additionally, fixed costs, variable costs and general costs are lower for on-site hydrogen production due to lower FCI as the air separation unit for generation of oxygen for gasification can be replaced by a single compressor for oxygen from electrolysis.

The operational result calculated as EBIT and EBT is summarized in Table 6. On-site production of hydrogen performs better than off-site generation of hydrogen due to lower TPC. However, the numbers clearly show that the hydrogen enhanced BtL process is unprofitable under current conditions, regardless if hydrogen is generated off-site or on-site. The reason are high costs for hydrogen from renewable energy produced by alkaline electrolysis. This can be attributed to alkaline electrolysis not yet being established on such a large scale.

3.2.3. Sensitivity analysis

Sensitivity analysis of the operational result shows the highest impact on TPC for cost of hydrogen (cf. Fig. 5) as could be expected from the large share of hydrogen costs from TPC. To a much smaller extent, FCI and market price of gasoline show the second highest sensitivity. This result leads to the conclusion that in the case evaluated the cost of product is primarily dependent on the cost of hydrogen while all other factors have a far lesser influence.

3.2.4. Discussion of economic process performance

The costs of hydrogen dominate the calculated TPC. The potential savings from local hydrogen production are not nearly high enough to have a significant effect on TPC. Hydrotreating of raw gasoline adds to high TPC as additional hydrogen is needed and equipment for hydrotreating requires a higher FCI compared to options where aromatics are separated or the gasoline from hydrogen enhanced MtG process is used as blending component. From sensitivity analysis, it can be concluded that above all a significant reduction of cost for hydrogen is needed for the hydrogen enhanced BtL process to become competitive. Depending on the site infrastructure, the use of available reactor waste heat from hydrogen enhanced MtG process for energy recovery could contribute to cost reduction by creating additional revenue from district heating, increased electricity generation, or use of process heat.

While the TPC cannot be compared directly due to different assumptions in economic analysis, these findings are backed by the results of Dietrich et al. [7] and Hannula [17] who also report the biggest impact on TPC being the cost of electricity for hydrogen production by electrolysis. However, a sharp reduction in cost for hydrogen would not be sufficient to break even. Even if hydrogen was provided at no charge (i.e. negative prices for electricity), TPC would be 0.82 €/kg fuel which still is above the assumed market price for gasoline and LPG under current conditions. Thus, additionally an increase of market prices for

Table 5
Estimation of total product costs and manufacturing costs in M€ per year for off- and on-site generation of hydrogen.

| Category	Item	Off-site H$_2$generation	On-site H$_2$generation
Fixed costs	Depreciation	79.8	73.8
	Taxes and insurance	35.9	33.2
	Interests on FCI and WC	44.0	40.7
Variable costs	Raw materials	1496.9	1481.1
	Straw	*120.0*	*120.0*
	Hydrogen	*1376.9*	*1361.1*
	Operating labor	29.6	29.6
	Utilities, consumables, logistics	92.2	81.8
	Maintenance	50.2	46.2
Plant overhead		39.9	37.9
Revenues by-product	Electricity	−30.9	−30.9
Manufacturing costs		**1837.5**	**1793.3**
General expenses		142.7	139.4
Total product costs		**1980.3**	**1932.7**
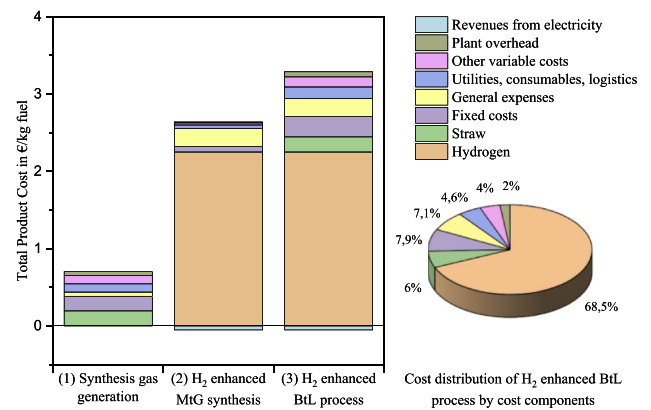
Fig. 4. Left: Total product costs in €/kg fuel for synthesis gas generation (pyrolysis and gasification) (1), hydrogen enhanced MtG process (off-site H$_2$ production) without synthesis gas generation (2), and complete process (hydrogen enhanced BtL process) (3). Right: Cost distribution by cost components on a percentage basis for hydrogen enhanced BtL process.

Table 6
Calculation of operational result of hydrogen enhanced BtL process as EBT and EBIT in M€.

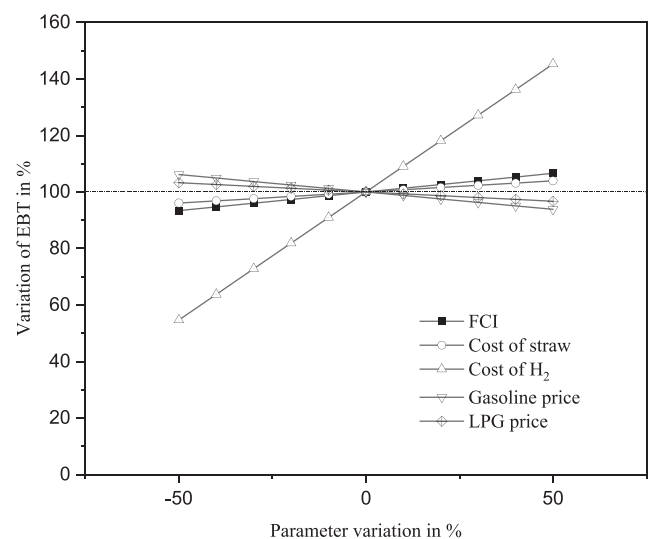|	Off-site H$_2$ generation	On-site H$_2$ generation
Total product costs	−1980.3	−1932.7
Revenues	307.4	307.4
Gasoline	*200.2*	*200.2*
LPG	*107.2*	*107.2*
EBT	**−1672.9**	**−1625.3**
Interests	44.0	40.7
EBIT	**−1628.8**	**−1584.6**

Fig. 5. Sensitivity analysis of EBT of hydrogen enhanced BtL process (off-site H$_2$ production) for main economic parameters.

LPG and gasoline from renewable sources, e.g. by imposing a tax on carbon dioxide emissions from fossil fuels, is necessary for the hydrogen enhanced BtL process to become profitable.

In comparison to the unmodified BtL process without feed-in of additional hydrogen modeled by Trippe et al. ([15,26]), the manufacturing costs are about twice as high. In contrast to this work, for the unmodified BtL process FCI has the highest impact on manufacturing costs. Only at a hydrogen price below 2.7 €/kg the hydrogen enhanced BtL process would

become competitive in comparison to the unmodified BtL process.

4. Conclusion

From an engineering perspective, the hydrogen enhanced BtL process is superior to the unmodified BtL process due to increased chemical and energy efficiency and higher carbon efficiency and thus product yield. However, economical analysis shows that the hydrogen enhanced BtL process is highly unprofitable under current conditions due to high costs for hydrogen provision from alkaline electrolysis. The TPC is dominated by the costs of hydrogen generation to such an extent that transportation costs of hydrogen and synergetic effects from local hydrogen generation do not have a significant effect. In comparison to the unmodified BtL process, the hydrogen enhanced BtL process only becomes economically favorable at hydrogen cost below 2.7 €/kg. Different catalysts that produce lower amounts of aromatic compounds

in hydrocarbon synthesis or a modified gasoline upgrading scheme with recovery of more valuable aromatics as benzene, toluene, and xylene could decrease TPC by reducing hydrogen consumption and decreasing FCI. To become economically competitive in comparison to fossil fuels a further reduction of hydrogen costs and higher market prices for gasoline and LPG are needed, e.g. by introducing an appropriate CO_2 tax.

Declaration of Competing Interest

None.

Acknowledgements

Appendix A
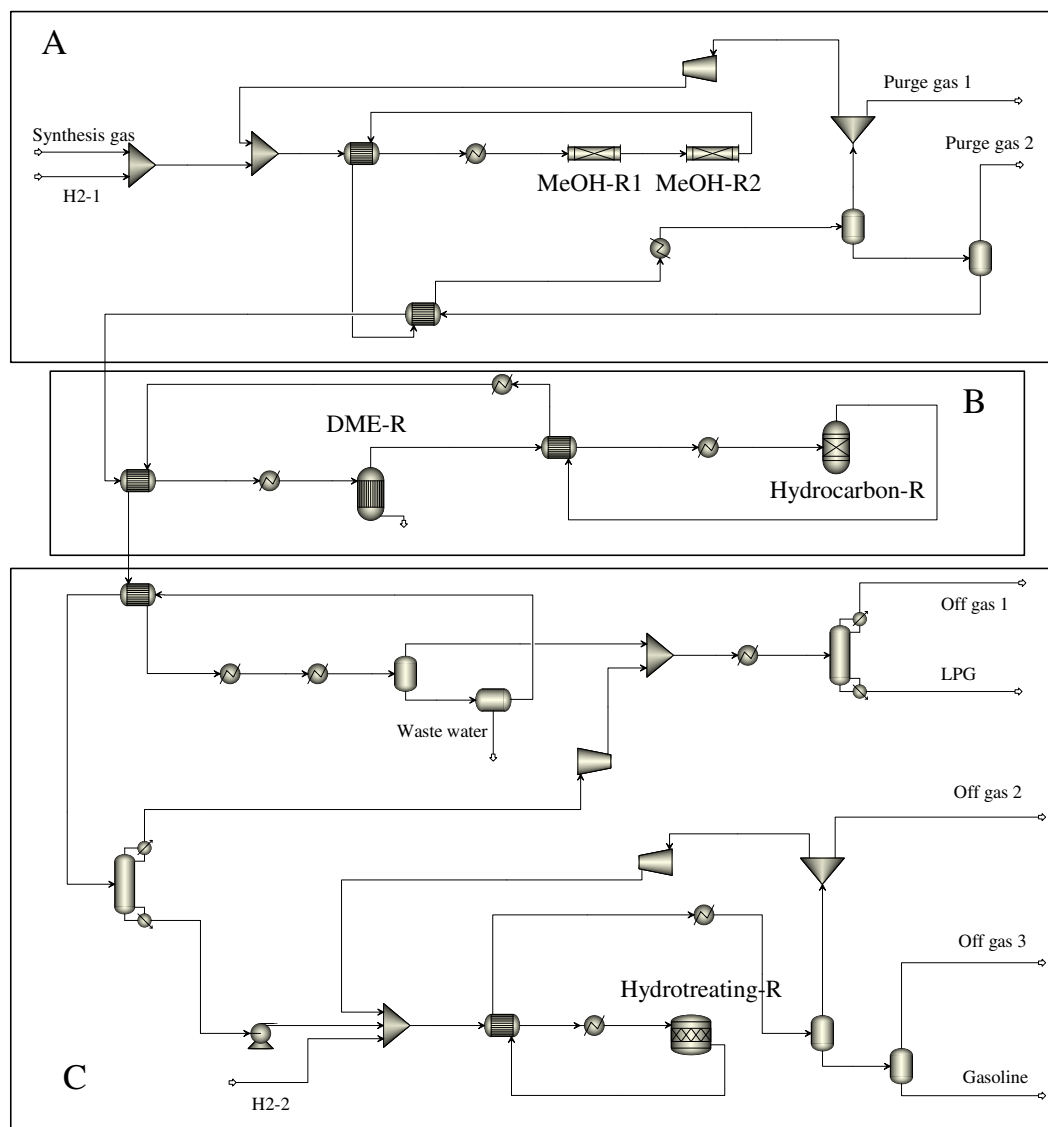
A.1. Aspen Plus process model

Fig. A1.1. Aspen Plus flowsheet of the hydrogen enhanced MtG process: (A) methanol synthesis, (B) hydrocarbon synthesis, (C) product recovery and purification.

A.2. Fixed Capital Investment (FCI)

Table A2.1

FCI of upstream processes (pyrolysis and gasification), hydrogen enhanced MtG synthesis (methanol synthesis, hydrocarbon synthesis, product recovery and purification), and downstream processes (CCGT) in M€ 2018.

Process steps/Components	Quantity	Capacity (total)	Unit	FCI in M€ 2018	
				H_2off-site	H_2on-site
Pyrolysis	11	284	t straw/h	422.9	
Gasification	1	1000	MW_{th}	438.6	347.3
Thereof					
Air separation unit and related components	1	105	t O_2/h	98.7	n.a.
Oxygen compressor (O_2 from electrolysis)	1	3.4	MW_e	n.a.	7.4
Methanol synthesis					
HX1	1	136	MW_{th}	34.7	
HX2	1	11	MW_{th}	1.8	
HX3	1	77	MW_{th}	7.8	
Methanol separator	1	747	t/h	5.2	
Methanol degasser	1	237	t/h	2.7	
Recycle compressor	1	5.1	MW_e	20.6	
Methanol reactor	4	224	t MeOH/h	35.3	
Hydrocarbon synthesis					
HX4	1	85	MW_{th}	9.4	
HX5	1	14	MW_{th}	1.4	
HX6	1	10	MW_{th}	0.8	
HX7	1	31	MW_{th}	2.4	
DME synthesis reactor beds	1	237	t/h	8.5	
DME synthesis reactor intercooler	1	7	MW_{th}	3.6	
Gasoline synthesis reactor beds	3 × 4	150	t DME-Equiv./h[a]	14.3	
Gasoline synthesis reactor intercooler	3 × 3	74	MW_{th}	45.1	
Product recovery and purification					
HX8	1	1	MW_{th}	0.1	
HX9	1	6	MW_{th}	0.7	
HX10	1	6	MW_{th}	0.5	
Raw product degassing	1	237	t/h	1.8	
Decanter	1	224	t/h	1.4	
Gasoline separator	1	55	t/h	0.7	
Gasoline degasser	1	52	t/h	0.6	
Raw product fractionation column	1	88	t/h	5.6	
LPG separation column	1	50	t/h	3.5	
LPG compressor	1	0.3	MW_e	4.5	
Hydrogenation recycle compressor	1	0.1	MW_e	5.3	
Raw gasoline pump	1	78	m^3/h	0.6	
Hydrogenation reactor	1	51	t raw gasoline/h	39.1	
CCGT					
Gas turbine	1	75	MW_e	34.0	
Steam generator	1	89	MW_{th}	20.5	
Steam turbine	1	24	MW_e	23.7	
Total FCI				1198	1106

[a] Calculated as DME for full conversion of MeOH

References

[1] International Energy Agency, Data and Statistics, IEA, 2020. Copyright: (c) 2020, https://www.iea.org/data-and-statistics?country=WORLD&fuel=Energy%20supply&indicator=Total%20primary%20energy%20supply%20(TPES)%20by%20source (last accessed 20.07.2020).

[2] United Nations, Climate Change. https://www.un.org/en/sections/issues-depth/climate-change/, 2020 (last accessed December 2020).

[3] European Parliament, Directive (EU) 2018/2001 of the European Parliament and of the Council of 11 December 2018 on the promotion of the use of energy from renewable sources, Off. J. Eur. Union (2018) 82–209.

[4] E. Henrich, N. Dahmen, E. Dinjus, J. Sauer, The role of biomass in a future world without fossil fuels, Chemie Ingenieur Technik 87 (12) (2015) 1667–1685.

[5] A. Sharma, A. Jakhete, A. Sharma, J.B. Joshi, V. Pareek, Lowering greenhouse gas (GHG) emissions: techno-economic analysis of biomass conversion to biofuels and value-added chemicals, Greenh. Gases 9 (3) (2019) 454–473.

[6] H. Kargbo, J.S. Harris, A.N. Phan, "Drop-in" fuel production from biomass: critical review on techno-economic feasibility and sustainability, Renew. Sust. Energ. Rev. 135 (2021) 110168.

[7] R.-U. Dietrich, F.G. Albrecht, S. Maier, D.H. König, S. Estelmann, S. Adelung, Z. Bealu, A. Seitz, Cost calculations for three different approaches of biofuel production using biomass, electricity and CO2, Biomass Bioenergy 111 (2018) 165–173.

[8] L. Faba, E. Díaz, S. Ordóñez, Recent developments on the catalytic technologies for the transformation of biomass into biofuels: a patent survey, Renew. Sust. Energ. Rev. 51 (2015) 273–287.

[9] M. Eberhard, U. Santo, B. Michelfelder, A. Günther, P. Weigand, J. Matthes, P. Waibel, V. Hagenmeyer, T. Kolb, The bioliq® entrained-flow gasifier–a model for the German Energiewende, Chem. BioEng. Rev. 7 (4) (2020) 106–118.

[10] N. Dahmen, J. Abeln, M. Eberhard, T. Kolb, H. Leibold, J. Sauer, D. Stapf, B. Zimmerlin, The bioliq process for producing synthetic transportation fuels, Wiley Interdisc. Rev. 6 (3) (2017).

[11] N. Dahmen, E. Henrich, E. Dinjus, F. Weirich, The bioliq® bioslurry gasification process for the production of biosynfuels, organic chemicals, and energy, Energy Sustain. Soc. 2 (3) (2012).

[12] R.G. dos Santos, A.C. Alencar, Biomass-derived syngas production via gasification process and its catalytic conversion into fuels by Fischer Tropsch synthesis: a review, Int. J. Hydrog. Energy 45 (36) (2020) 18114–18132.

[13] M. Iglesias Gonzalez, B. Kraushaar-Czarnetzki, G. Schaub, Process comparison of biomass-to-liquid (BtL) routes Fischer–Tropsch synthesis and methanol to gasoline, Biomass Convers. Biorefinery 1 (4) (2011) 229.

[14] P. Chiesa, S. Consonni, T. Kreutz, R. Williams, Co-production of hydrogen, electricity and CO2 from coal with commercially ready technology. Part A: Performance and emissions, Int. J. Hydrog. Energy 30 (7) (2005) 747–767.

[15] F. Trippe, M. Fröhling, F. Schultmann, R. Stahl, E. Henrich, A. Dalai, Comprehensive techno-economic assessment of dimethyl ether (DME) synthesis and Fischer–Tropsch synthesis as alternative process steps within biomass-to-liquid production, Fuel Process. Technol. 106 (2013) 577–586.

[16] H. Gruber, P. Groß, R. Rauch, A. Reichhold, R. Zweiler, C. Aichernig, S. Müller, N. Ataimisch, H. Hofbauer, Fischer-Tropsch products from biomass-derived syngas and renewable hydrogen, Biomass Convers. Biorefinery (2019) 1–12.

[17] I. Hannula, Hydrogen enhancement potential of synthetic biofuels manufacture in the European context: a techno-economic assessment, Energy 104 (2016) 199–212.

[18] C. Panzone, R. Philippe, A. Chappaz, P. Fongarland, A. Bengaouer, Power-to-Liquid catalytic CO2 valorization into fuels and chemicals: focus on the Fischer-Tropsch route, J. CO2 Utilization 38 (2020) 314–347.

[19] T. da Silva Veras, T.S. Mozer, A. da Silva César, Hydrogen: trends, production and characterization of the main process worldwide, Int. J. Hydrog. Energy 42 (4) (2017) 2018–2033.

[20] S.E. Hosseini, M.A. Wahid, Hydrogen production from renewable and sustainable energy resources: promising green energy carrier for clean development, Renew. Sust. Energ. Rev. 57 (2016) 850–866.

[21] C. Wulf, M. Kaltschmitt, Hydrogen supply chains for mobility—environmental and economic assessment, Sustainability 10 (6) (2018) 1699.

[22] IEA, Hydrogen Projects Database. https://www.iea.org/reports/hydrogen-projects-database, IEA, Paris, .

[23] G. Glenk, S. Reichelstein, Economics of converting renewable power to hydrogen, Nat. Energy 4 (3) (2019) 216–222.

[24] F. Trippe, M. Fröhling, F. Schultmann, R. Stahl, E. Henrich, Techno-economic analysis of fast pyrolysis as a process step within biomass-to-liquid fuel production, Waste Biomass Valorization 1 (4) (2010) 415–430.

[25] F. Trippe, M. Fröhling, F. Schultmann, R. Stahl, E. Henrich, Techno-economic assessment of gasification as a process step within biomass-to-liquid (BtL) fuel and chemicals production, Fuel Process. Technol. 92 (11) (2011) 2169–2184.

[26] F. Trippe, Techno-ökonomische Bewertung alternativer Verfahrenskonfigurationen zur Herstellung von Biomass-to-Liquid (BtL) Kraftstoffen und Chemikalien, KIT Scientific Publishing, 2013.

[27] C. Wulf, P. Zapp, Sustainability assessment of innovative energy technologies – Hydrogen from wind power as a fuel for mobility applications, in: 14th Conference on Sustainable Development of Energy, Water and Environment Systems (SDEWES), October 1–6, Dubrovnik, Croatia, Book of Abstracts, 2019.

[28] C. Wulf, M. Reuß, T. Grube, P. Zapp, M. Robinius, J.-F. Hake, D. Stolten, Life Cycle Assessment of hydrogen transport and distribution options, J. Clean. Prod. 199 (2018) 431–443.

[29] M. Haase, C. Rösch, Sustainability assessment of innovative energy technologies - Integrated biomass-based production of fuel, electricity and heat, in: ETA-Florence Renewable Energies (Hrsg.): Proceedings of the 27th European Biomass Conference and Exhibition, Lisbon, Portugal, 27.-30.05.2019, ETA-Florence Renewable Energies, Florenz, Italien, 2019, 2019, publ. online, S. 1642–1653.

[30] J. Ott, V. Gronemann, F. Pontzen, E. Fiedler, G. Grossmann, D.E.A. Kersebohm, Methanol, in: Ullmann's Encyclopedia of Industrial Chemistry, Wiley, Chichester, 2010, p. 197.

[31] H. Modarresi, Methanol synthesis process layout for large production capacity, International Application Published Under the Patent Cooperation Treaty (PCT), International Publication Number WO2017/167642Al, Google Patents, 2017.

[32] S. Kvisle, T. Fuglerud, S. Kolboe, U. Olsbye, K.P. Lillerud, B.V. Vora, Methanol-to-hydrocarbons, in: Handbook of Heterogeneous Catalysis, Wiley-VCH Verlag GmbH & Co. KGaA, Weinheim, Germany, 2008, pp. 2950–2965.

[33] S. Lee, M. Gogate, C.J. Kulik, Methanol-to-gasoline vs. dme-to-gasolne II. process comparison and analysis, Fuel Sci. Technol. Int. 13 (8) (1995) 1039–1057.

[34] C.D. Chang, Hydrocarbons from methanol, Catal. Rev. Sci. Eng. 25 (1) (1983) 1–118.

[35] E.C. Tan, M. Talmadge, A. Dutta, J. Hensley, L.J. Snowden-Swan, D. Humbird, J. Schaidle, M. Biddy, Conceptual process design and economics for the production of high-octane gasoline blendstock via indirect liquefaction of biomass through methanol/dimethyl ether intermediates, Biofuels Bioprod. Biorefin. 10 (1) (2016) 17–35.

[36] Aspen Technology, Aspen Physical Property Methods: Peng Robinson Alpha Functions, Aspentech, Cambridge, USA, 2020.

[37] K.V. Bussche, G. Froment, A steady-state kinetic model for methanol synthesis and the water gas shift reaction on a commercial Cu/ZnO/Al2O3Catalyst, J. Catal. 161 (1) (1996) 1–10.

[38] É.S. Van-Dal, C. Bouallou, Design and simulation of a methanol production plant from CO2 hydrogenation, J. Clean. Prod. 57 (2013) 38–45.

[39] C.D. Chang, A.J. Silvestri, The conversion of methanol and other O-compounds to hydrocarbons over zeolite catalysts, J. Catal. 47 (2) (1977) 249–259.

[40] T. Michler, N. Wippermann, O. Toedter, B. Niethammer, T. Otto, U. Arnold, S. Pitter, T. Koch, J. Sauer, Gasoline from the bioliq® process: production, characterization and performance, Fuel Process. Technol. 206 (2020) 106476.

[41] F.J. Keil, Methanol-to-hydrocarbons: process technology, Microporous Mesoporous Mater. 29 (1–2) (1999) 49–66.

[42] DIN EN 228 Automotive fuels – Unleaded petrol – Requirements and test methods; German version EN 228:2012+A1:2017, Deutsches Institut für Normung (2017).

[43] M. Wilson, I. Fisher, J. Kriz, Hydrogenation and extraction of aromatics from oil sands distillates and effects on cetane improvement, Energy Fuel 1 (6) (1987) 540–544.

[44] J.C. Koj, C. Wulf, A. Schreiber, P. Zapp, Site-dependent environmental impacts of industrial hydrogen production by alkaline water electrolysis, Energies 10 (7) (2017) 860.

[45] M.S. Peters, K.D. Timmerhaus, R.E. West, Plant Design and Economics for Chemical Engineers, McGraw-Hill, University of Colorado, 2004.

[46] Kuratorium für Technik und Bauwesen in der Landwirtschaft e. V. (KTBL), KTBL-Feldarbeitsrechner. https://daten.ktbl.de/feldarbeit/entry.html, 2020.

[47] L. Leible, S. Kälber, G. Kappler, Systemanalyse zur Gaserzeugung aus Biomass Untersuchung ausgewählter Aspekte: Biomasseaufkommen und -bereitstellung, Biomasseeinspeisung in einen Druckvergaser, Verfahrensvergleich der FT- und Methanolproduktion, KIT Scientific Publishing Karlsruhe, 2011.

[48] European Energy Exchange AG, KWK Index, Available from, https://www.eex.com/de/marktdaten/strom/kwk-index, 2020 (last accessed August 18, 2020).

[49] J. Michels, Pilotprojekt Lignocellulose-Bioraffinerie: Gemeinsamer Schlussbericht zu den wissenschaftlich-technischen Ergebissen aller Teilvorhaben, DECHEMA, 2009.

[50] W. Li, Q. Dang, R. Smith, R.C. Brown, M.M. Wright, Techno-economic analysis of the stabilization of bio-oil fractions for insertion into petroleum refineries, ACS Sustain. Chem. Eng. 5 (2) (2017) 1528–1537.

[51] Mineralöl Wirtschaftsverband e.v. (MWV), Zusammensetzung des Verbraucherpreises für Superbenzin, Available from, https://www.mwv.de/statistiken/preiszusammensetzung/, 2020 (last accessed February 12, 2020).

[52] BOVAG-RAI Foundation, Mobility in Figures: Cars 2018–2019, 2019.

[53] M. Pérez-Fortes, E. Tzimas, Techno-Economic and Environmental Evaluation of CO2 Utilisation for Fuel Production, JRC Science Hub, ZG Petten, The Netherlands, 2016.

[54] Verband der chemischen Industrie e.v, Chemiewirtschaft in Zahlen, VCI, Frankfurt, 2020.

[55] Statista, Jährliche Entwicklung des Wechselkurses des Euro gegenüber dem US-Dollar von 1999 bis 2019, Available at, https://de.statista.com/statistik/daten/studie/200194/umfrage/wechselkurs-des-euro-gegenueber-dem-us-dollar-seit-2001/, 2019 (last accessed December 12, 2019).

[56] E.C. Tan, M. Talmadge, A. Dutta, J. Hensley, J. Schaidle, M. Biddy, D. Humbird, L. J. Snowden-Swan, J. Ross, D. Sexton, Process Design and Economics for the Conversion of Lignocellulosic Biomass to Hydrocarbons via Indirect Liquefaction. Thermochemical Research Pathway to High-Octane Gasoline Blendstock Through Methanol/Dimethyl Ether Intermediates, National Renewable Energy Lab.(NREL), Golden, CO (United States), 2015.

[57] E.D. Larson, H. Jin, F.E. Celik, Gasification-Based Fuels and Electricity Production from Biomass, without and with Carbon Capture and Storage, Princeton Environmental Institute, Princeton University, 2005.

[58] G. Wöhe, U. Döring, Einführung in die allgemeine Betriebswirtschaftslehre, Vahlen, München, 2002.